INTERNATIONAL JOURNAL OF AUTOMOTIVE SCIENCE AND TECHNOLOGY

2024, VOL. 8, NO:3, 387-396 www.ijastech.org e-ISSN: 2587-0963

# Effect of Design Parameters on Buckling Tendency of an Eccentric Drag Link Used in a Truck Steering Linkage: A DoE/RSM-Based Design Optimisation Study

Kübra Polat[1*], Mehmet Murat Topaç[1*] and Ufuk Çoban[2]

[1.] *Mechanical Engineering Department, Faculty of Engineering, Dokuz Eylül University, Izmir, 35397, Türkiye*

[2.] *BMC Automotive Industry and Trade Inc., Heavy Commercial Vehicles Division, Bornova, Izmir, 35060, Türkiye*

**Abstract**

The steering system, deemed one of the most critical subsystems for ensuring the safety of a vehicle, is characterised by its pivotal role in manoeuvrability and control. The primary function of transmitting the steering input from the steering wheel to the vehicle's wheels is carried out by the drag link within the steering system. Therefore, the durability and proper functioning of the drag link in vehicles, especially carrying heavy loads, are of critical importance for both safety and efficiency. The main purpose of this study is to determine the optimal geometry of the drag link utilised in the steering system of a 4x2 truck using the Design of Experiments-Response Surface Methodology (DoE-RSM). Firstly, an idealised worst-case load model was used to determine the maximum force applied by the Pitman arm on the drag link. The stress distribution and deformation on the drag link caused by the maximum design load were determined using Finite Element Analysis (FEA). Based on the results of the analyses, eccentricity, rod thickness, and fillet radius were defined as design parameters. The parameter ranges were determined by considering the volume swept by the wheel and buckling criteria under maximum load conditions. According to the DoE-RSM results, concerning the local sensitivity percentages of the parameters on total deformation, it was observed that the eccentricity (e) parameter has the most significant impact, with an approximate positive rate of 74%.

*Keywords*: Commercial Vehicle; Finite Element Analysis; Optimization; Steering System; Structural Design

**Research Article**

**History**
Received 15.05.2024
Revised 19.07.2024
Accepted 18.09.2024

**Contact**
* Corresponding author
Kübra Polat
k.polat@ogr.deu.edu.tr
Address: Mechanical Engineering Department, Faculty of Engineering, Dokuz Eylül University, Izmir, Türkiye
Tel: +902323019248

***To cite this paper***: Polat, K., Topaç, MM., Çoban, U., Effect of Design Parameters on Buckling Tendency of an Eccentric Drag Link Used in a Truck S teering Linkage: A DoE/RSM-Based Design Optimisation Study. International Journal of Automotive Science and Technology. 2024; 8(3): 387-396. https://doi.org/10.30939/ijastech..1484736

## 1. Introduction

The steering system is one of the most critical subsystems of a land transport vehicle regarding safety [1]. The general view and the mechanical components of a steering linkage used in a tractor truck can be seen in Figure 1 [2]. These components can be listed as the steering shaft, steering gearbox, pitman arm, drag link, steering arm, track rod, and tie rod. The steering torque input applied to the steering wheel is transferred to a gear system known as the steering box, through the steering shaft. Afterward, by means of a Pitman arm connected to the output shaft of the gearbox, the steering motion is transmitted to the drag link and the steering arm connected to the stub axle, enabling the vehicle's wheels to turn right or left for steering. The transmission of the steering motion between the axle wheels is provided by the tie rod. Due to its function of transferring the applied steering torque to the wheels, the drag link stands out as a vital structural component of this system [3,4].

On the other hand, in many steering system applications, the volume in which the wheel operates (wheel envelope) does not allow for the linear rod-shaped design of the rod. Therefore, in the production of these rods, they are subjected to bending at certain points in addition to tensile or compressive loading [5]. In this case, the eccentric design of the component becomes inevitable. This also results in the generation of an additional bending moment due to the axial forces acting on the component during the transmission of steering torque. Therefore, during the design stage, it is necessary to assess the component in terms of buckling as well [3,6]. The mechanical and buckling behaviour of the drag link under various loading conditions has been investigated in detail by various studies in the literature. Finite Element Analyses (FEA) were performed for different rod materials to investigate the buckling strength of drag link with optimum performance for a heavy-duty vehicle in [7] and [8]. In another study, structural analysis was carried out to evaluate the durability of steering components under various loading conditions. In addition, the buckling strength of the drag link was also

investigated [9]. Vijaykumar and Anand applied FEA for a high strength drag link and the buckling strength of the rod was calculated using the available material properties. Subsequently, buckling strength tests were carried out on three specimens [4].

None of these studies concentrate to evaluate the effects of design factors on buckling safety of an eccentric drag link.

a

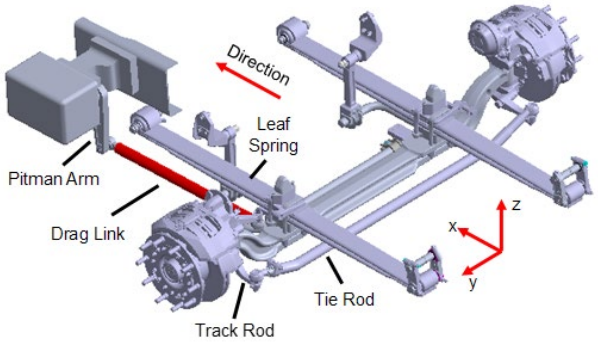


b

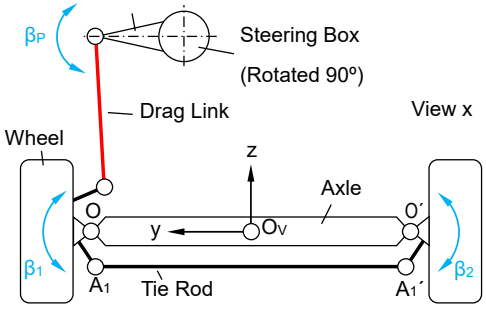


c

Fig. 1.a. An exemplary truck tractor [10] b. The steerable front axle of a truck, c. Kinematic representation from the front view [2]

In the scope of this study, the method mentioned in the literature [3] was employed for the design of the drag link used in the steering system of a 4x2 drivetrain configuration commercial truck. Firstly, the total moment for the worst case of the system was calculated using the idealised method [1,2]. Subsequently, FEA was applied to the steering system using this moment to determine the most severe steering condition. A parametric model of the drag link was built and three design parameters were determined. These are eccentricity (e), corner radius (R) and pipe wall thickness (t). The range of values for these parameters was determined by considering the wheel envelope and the buckling safe region. Then, the Design of Experiments - Response Surface Methodology (DoE-RSM) was used to examine the effects of these parameters on stress and total deformation and to determine the optimal values for the component. As a result of this parametric study, the effect percentages of the chosen design parameters were determined and their importance in the design stage was identified. The reliability of the design created with the obtained parameters was also evaluated in terms of buckling stability. The FEA of the final design of the drag link geometry showed that it is safe in terms of material and also in the safe region according to various buckling criteria. To the best of the authors' knowledge, there is no literature in which the effect of drag link eccentricity on the design geometry and strength of the part has been analysed in detail. The studies carried out within the scope of this study have determined the design parameters that should be considered in drag link design. The effects of these design parameters on part performance are also analysed in this study. In general, the part design steps are summarised.

## 2. Material and method

### 2.1 Load model

In this study, the critical loading condition was assumed as the wheel is steered without rolling [2,11]. In this loading condition shown in Figure 2, it is assumed that, in addition to the vertical load G, the bore torque ($M_B$), which arises as resistance against steering and is presumed to act in the plane of the road from the centre point F' of the tyre contact patch [2,12,13]. The bore torque ($M_B$) was calculated using an idealised model proposed by Rill [2]. According to this model, the wheel-road contact surface can be idealised as an approximate rectangular surface with edge lengths B and L, while under a specific vertical load. The area of this contact surface is considered equivalent to the area of a circle with the radius $R_B$, as shown in Figure 2(b). Here, the vertical stiffness of the tyre ($C_R$) directly affects B and L.

The equivalent circle radius is calculated as follows:

$$R_B = \frac{1}{4}(L+B) \tag{1}$$

B is considered approximately equal to the tyre width. The dimensions of the wheels used in the vehicle are 295/80 R 22.5. $M_B$ is calculated as follows:

$$M_B = \frac{2}{3} R_B F \tag{2}$$

where, F is the friction force acting on a unit surface element. In this model the scrub radius is neglected.

In order to obtain the highest possible stress concentration on the rod, the coefficient of adhesion between the road and the wheel

is assumed as $\mu_H \approx 1$ [14]. The above calculations were performed for both wheels, and the total moment that the pitman arm must overcome was found.

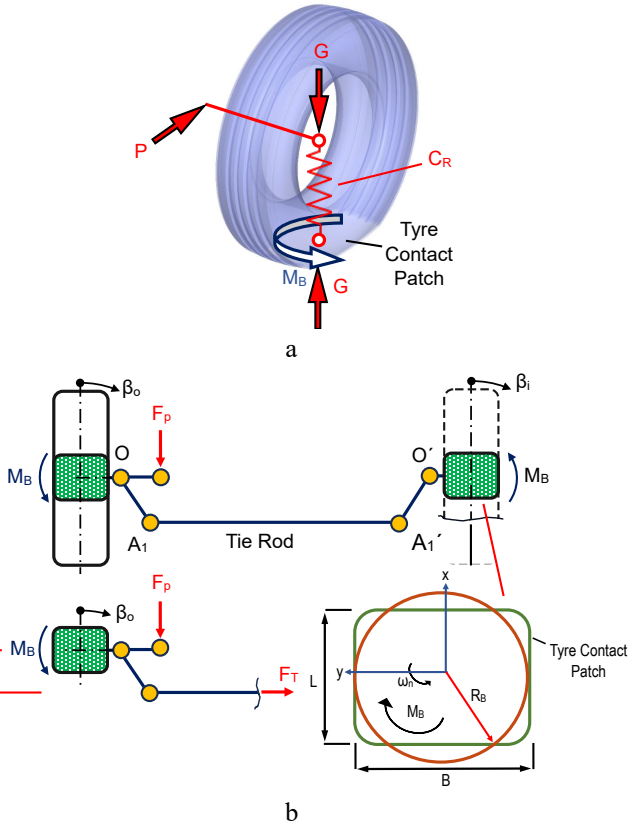


Fig. 2.a. Schematic representation of the critical loading condition
b. Model idealised by Rill [2]

### 2.2 Buckling of a beam with eccentricity

In axial loaded parts, the force direction and the axis of the component are rarely overlap in practice. In most engineering applications, the effect of eccentricity also needs to be taken into account. In Figure 3, schematic of an eccentrically loaded part under a specific "e" eccentricity is illustrated [3, 15].

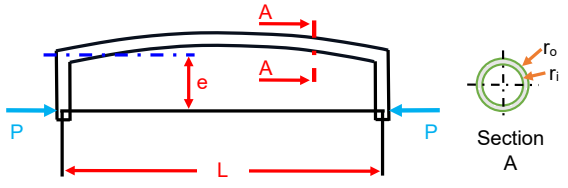


Fig. 3.Eccentrically loaded structural element (according to [14])

The relationship between the force (P) acting eccentrically on the structural member and the resulting moment (M) can be expressed as follows:

$$M = P.\, e \tag{3}$$

Here, 'e' is the eccentricity distance from the neutral axis of the rod. To prevent plastic deformation, the calculated maximum buckling stress ($\sigma_{max}$) value must be equal to or less than the material's yield stress ($\sigma_y$). In the case of $\sigma_{max} > \sigma_y$, the structure may go out of the elastic state and undergo plastic deformation resulting in damage. Therefore, when analysing the behaviour of eccentric parts, it is necessary to consider the situation where the stress in the critical section of the material reaches its maximum value. In the assessment of buckling for eccentric rods, various methods are available. One of the commonly used methods among these is the secant formula, expressed as follows [15]:

$$\sigma_{max} = \frac{P}{A}\left(1 + \frac{ec}{r^2} sec \frac{L}{r}\sqrt{\frac{P}{4EA}}\right) \tag{4}$$

or

$$\sigma_{max} = P\left(\frac{1}{A} + \frac{ec}{I} sec \frac{\pi}{2}\sqrt{\frac{P}{P_{cr}}}\right) \tag{5}$$

Here, P represents the axial load; L is the length of the rod; r is the minimum radius of gyration; e is the eccentricity of the rod; E is the modulus of elasticity of the material; and c is the farthest point from the neutral axis of the cross-section. The ratio L/r in the equation is referred to as the slenderness ratio, where r can be expressed as:

$$r = \sqrt{\frac{I}{A}} \tag{6}$$

Design with higher slenderness ratio is more prone to damage. A commonly used approach for design of columns operating under axial load is the American Institute of Steel Construction (AISC) criterion. This criterion can be summarized as follows [3,16,17]:

$$\sigma_{cr} = \left(0.658^{\frac{\sigma_y}{\sigma_e}}\right)\sigma_y \qquad \frac{L}{r} < 4.71\sqrt{\frac{E}{\sigma_Y}} \tag{7}$$

or

$$\sigma_{cr} = (0.877)\sigma_e \qquad \frac{L}{r} > 4.71\sqrt{\frac{E}{\sigma_Y}} \tag{8}$$

In these equations, $\sigma_y$ represents the yield stress, and $\sigma_e$ represents the Euler stress. $\sigma_e$ is expressed by the following equation:

$$\sigma_e = \frac{\pi^2 E}{\left(\frac{L}{r}\right)^2} \tag{9}$$

As seen in Eq. (7), an exponential expression is used to predict the buckling stress for short and intermediate-length columns, while a Euler-based relationship is utilized for long columns. These equations do not include a safety factor, therefore, a safety factor needs to be added to obtain AISC design formulas. During design, it is recommended to consider a safety factor of 1.67 and the allowable stress $\sigma_{all}$ is expressed by the following equation:

$$\sigma_{all} = \frac{\sigma_{cr}}{1.67} \tag{10}$$

The safety condition in this approach is as follows:

$$\frac{P}{A} + \frac{Pec}{I} \leq \sigma_{all} \tag{11}$$

### 2.3 Design of Experiments -Response Surface Method

In the open literature, there are a plenty of studies focusing on the determination of stress concentration regions on mechanical components. FE-based optimisations are also frequently used for design improvement [3,12,14,18-20]. DoE and RSM are commonly used methods in engineering and statistics for optimizing the performance of a system or process. These approaches are used together to examine the relationship between design variables (also known as input parameters) and the system's response (also known as output parameters). DoE produces appropriate design points (experiments) to examine the effect of more than one variable in the system on the response in a systematic way and produces a model of the behaviour of the system through the systemic responses of these points under various system inputs. This method assists researchers in identifying the most significant variables and determining their optimal levels for maximum performance. RSM is a statistical approach that attempts to explain the relationship between input variables and output variables using mathematical models. This method can be used to predict the system's response based on the levels of input variables and optimise the system's performance by determining the optimal levels of input variables. While the DoE approach is used to understand the relationship between the design parameters of the system and its performance, the main objective of the RSM is to predict and analyse the relationship between design variables and system response to obtain an appropriate model [21]. To create a model that explains the relationship between design variables and the system response, response surface experiments designed according to specific rules are required. Through the results obtained from these experiments, the effects of design variables on the system response can be determined, and a mathematical model can be created using this information. The regression model for a second-order response surface can be defined as follows [21]:

$$y = \beta_0 + \sum_{i=1}^{k} \beta_i x_i + \sum_{i \le j}^{k} \beta_{ij} x_i x_j + \varepsilon \quad (12)$$

or in matrix form, this relationship can be expressed as:

$$y = X\beta + \varepsilon \quad (13)$$

takes the form. Here, y is the observation vector, X is the model matrix, β is the vector containing partial regression constants, and ε is the error vector [21]. In this study, DoE and RSM were employed to determine the impact of specific parameters that constitute the geometry of the eccentric drag link on the elastic stability properties of the component. Figure 4 illustrates the methodology [21].

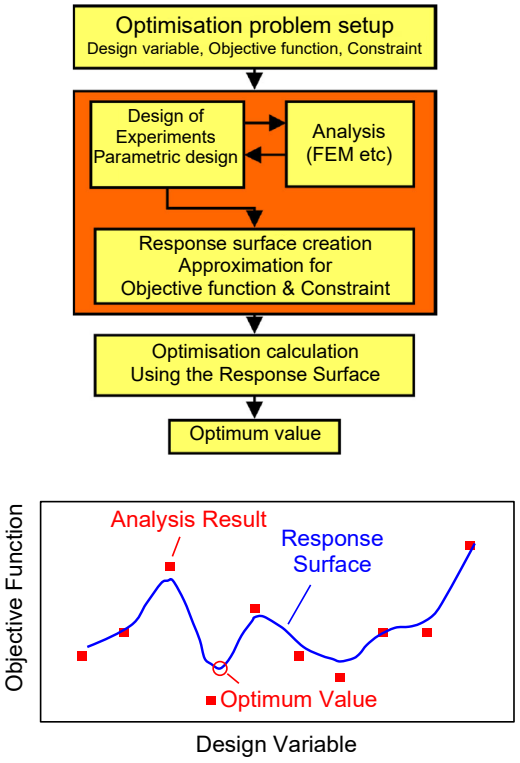


Fig. 4.Optimisation methodology [21]

## 3. Results and discussion

### 3.1 Design constraints and preliminary design

The wheel angles during a steering manoeuvre were determined using the Ackermann principle. During the turning motion of the vehicle, all wheels move on a curvature. To maintain steering stability and ensure minimal tire wear, the wheels need to roll without slipping. This condition where the instantaneous centres of rotation of the wheels coincide is called the "Ackermann geometry" and can be expressed as follows [1,22]:

$$\tan \beta_i = \frac{L}{R - \frac{w}{2}} \quad \text{and} \quad \tan \beta_o = \frac{L}{R + \frac{w}{2}} \quad (14)$$

Here, $\beta_i$ represents the steering angle of the inner wheel, and $\beta_o$ represents the steering angle of the outer wheel. The angles for the inner and outer wheels are defined concerning a turning centre marked as O in Figure 5(a). The distance between the steering axes of the steerable wheels is referred to as the track width and is denoted by 'w.' The wheelbase is represented as L [1]. The angular positions of the inner and outer wheels, calculated for different turning radii with Eq. (14), are illustrated in Figure 5(b). The turning angles of the inner wheel and outer wheels were obtained as 46° and 33° respectively based on the given vehicle dimensions and the desired minimum turning radius, which is denoted as Rs.

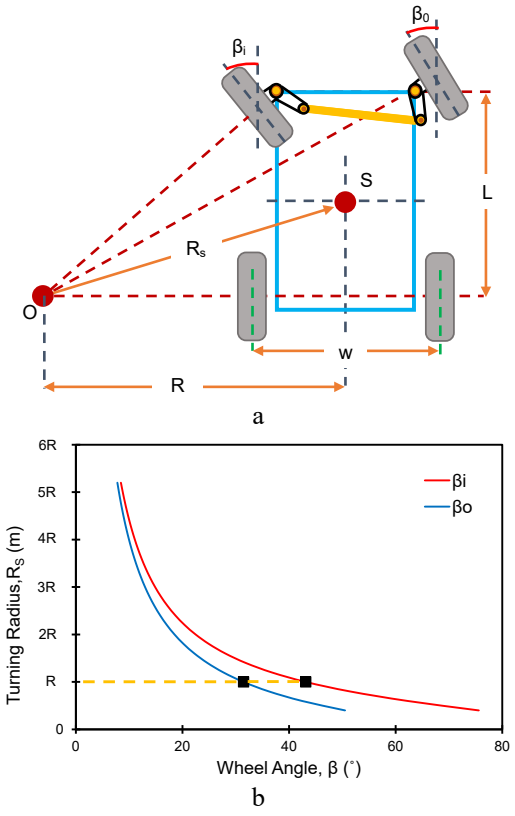


Fig. 5.a. The Ackermann condition, b. The angles of the inner and outer wheels for different turning radii

Considering the calculated angle values, the volume swept by the wheel was taken into account between full right and full left manoeuvres, and it was observed that the penetration of drag link with the wheel occurs at this angle. Within the scope of this study, the impact of shifting the steering gearbox position in –y axis was also investigated with the aim of obtaining a linear drag link and eliminate the need for eccentricity. As a result of repositioning the Pitman arm in –y axis, a difference of 1.12˚ in the maximum possible steering angle of the outer wheel was observed. This difference increases the minimum turning radius by approximately 7%, thereby reducing the manoeuvrability of the vehicle. In this case, the addition of eccentricity to the component is required during the design stage to achieve more effective steering. Thus, the approximate range for the minimum eccentricity value that should be possessed by the steering component was determined. The wheel envelope is illustrated in Figure 6.

The initial geometry of the drag link to be used in the steering system was determined by taking the wheel operating envelope into account. Eccentricity is affected by changes in the steering range of the front wheels. In the steering geometry employed in this study, the wheel operating angle of 32˚ is critical. This is because, for angle values lower than this limit, the steering linkage component can be designed as a linear hollow bar, whereas, for angle values higher than 32˚, it becomes necessary to introduce an eccentricity to the component.

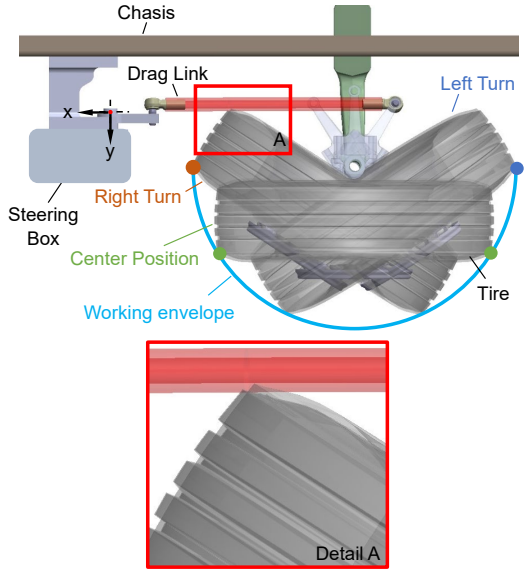


Fig. 6.The working envelope is determined by wheel turning angles and the interference zone in the absence of eccentricity

The variation above the critical angle alters the eccentricity value that needs to be applied to the component to a certain extent. As the wheel operating angle increases, the eccentricity applied to the drag link also increases. This relationship is illustrated in Figure 7.

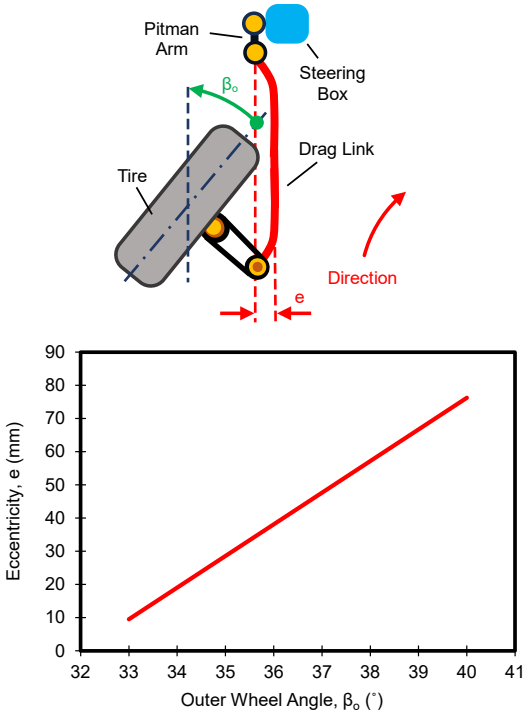


Fig. 7.The variation of eccentricity concerning the wheel angle

P460 steel was chosen for the manufacturing of the drag link. A detailed summary of the mechanical properties of the P460 material is presented in Table 1.

In the initial stage of the design, the outer diameter ($d_0$) of the drag link was selected to minimise penetration issues during production. For this purpose, the volume swept by the wheel between full right and full left manoeuvres were taken into account. Thus, the required eccentricity of the drag link was approximately determined. For this reason, the larger the outer diameter of the drag link was selected, the required eccentricity also increases proportionally according to Figure 6.

Table 1. Mechanical properties of the drag link material

| Mechanical Properties | Value |
|---|---|
| Modulus of Elasticity, E (GPa) | 200 |
| Poisson ratio | 0.3 |
| Tensile Strength, $R_m$ (MPa) | 560-730 |
| 0.2% strength ($R_{p0.2}$) (MPa) | 460 |

This is not a desired condition. The allowed maximum eccentricity value for the component is determined by the critical buckling value at which the component begins to fail. Thus, the component was safely designed against buckling by all criteria [3, 16,17]. The graphical representation of the maximum stress value as a function of the slenderness ratio (L/r) is shown in Figure 8.

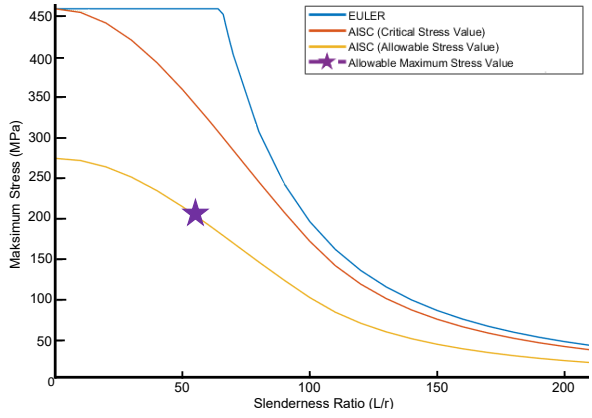


Fig. 8.The variation of the maximum stress concerning the slenderness ratio according to different criteria

### 3.2 Finite Element Model

The physical model created for performing FEA of the steering subsystem consists of one drag link, one steering knuckle, and two spherical joints. In this model, the chassis and steering box were connected by means of a bracket. The connections of the drag link were defined as spherical joint. The rotation of the wheel group around the kingpin axis was allowed. Here, the kingpin inclination was neglected. In the analysis, it is assumed that the steering torque applied to the system from the pitman's arm exactly counteracts the total resistance torque of the front wheels. SOLID187 element consisting of a total of ten nodes with three linear degrees of freedom each was used in the FE model of the drag link. This model consists of 62,744 elements and 108,700 nodes. The model, created by the connection constraints mentioned above, is shown in Figure 9.

In order to determine the worst case where of the pitman arm force acting on the drag link reaches its maximum value, five different angular positions of the arm were determined as follows 0˚ (centre position), 15˚, 33˚, -15˚, and -31˚. Here, negative and positive signs represent left and right turn manoeuvres respectively. FEA were conducted by taking these positions into account. The normalised reaction forces obtained from the analyses, which are shown in Figure 9(b), are proportionally expressed concerning the centre position (0˚) as a reference point. Here, the axial force acting on the arm for the central position ($F_0$) is assumed as 1. The analysis results showed that the maximum axial force (F) occurs during the wheel's maximum right turn manoeuvre.

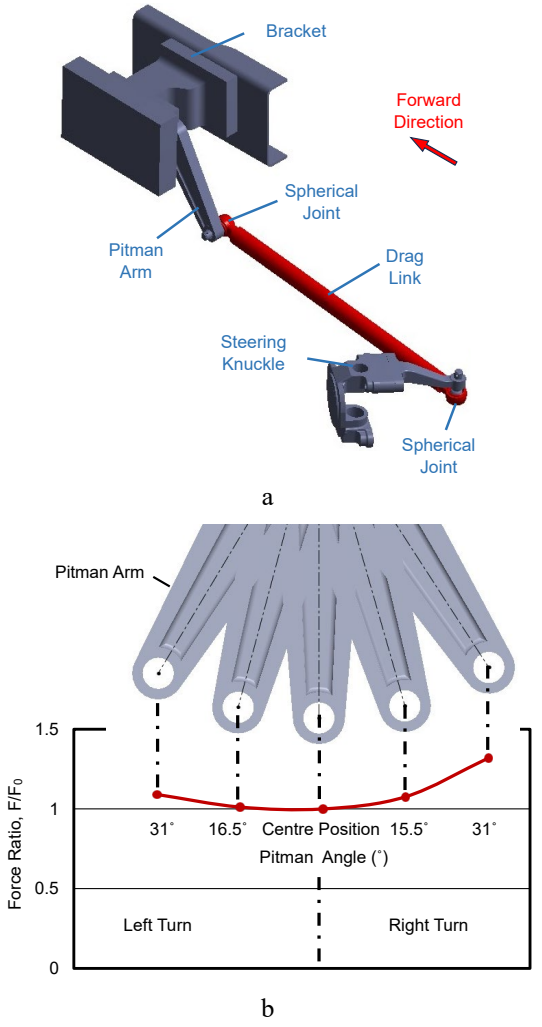


Fig. 9.a. The Finite Element model (right turn), b. Five different angle positions of the Pitman's arm and axial force variation according to the centre position

### 3.3 Parametric optimisation

The preliminary design of the drag link was initially made in the form of a hollow rod. However, since the rod shape cannot

be linear due to the wheel operating envelope, a very low initial eccentricity "e" was given to the part at the initial stage. A FEA was performed according to the worst-case scenario shown in Figure 9. According to the results of the analyses, it was seen that the difference between the stress concentration region in a linear and eccentric geometry is in the eccentricity area, which is shown as Region B in Figure 10.

In order to reduce the stress intensity, certain input parameters were selected on the rod and an optimum design search was carried out according to the total deformation and stress values. For this purpose, the rod was designed in accordance with the DoE module and DoE was carried out depending on the determined parameters. The design parameter values to minimise the stress intensity and total deformation were determined by creating response surfaces with the output parameters obtained using the DoE results.

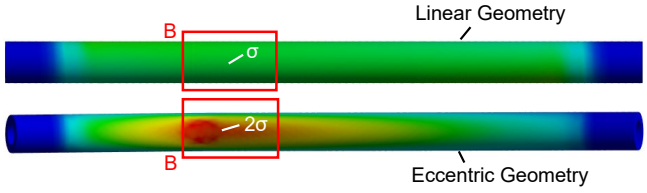


Fig. 10. SEA results of the preliminary design

The eccentricity was determined as the first design parameter. The second parameter was chosen as the tube wall thickness, t and the third parameter were determined as the curve radius R as shown in Figure 11(a). An analysis model was developed for the application of DoE, based on the calculated torque and the selected worst-case scenario. In this newly created model, the connection bracket and wheel connection were not used. Additionally, the solid models of spherical joints were also removed, and their functions on the component were simulated with joint definitions. The axial force was applied in the form of the critical load obtained from the analysis results. The parameters determined within the scope of the study and the FEA model created for the DoE study are shown in Figure 11(b).

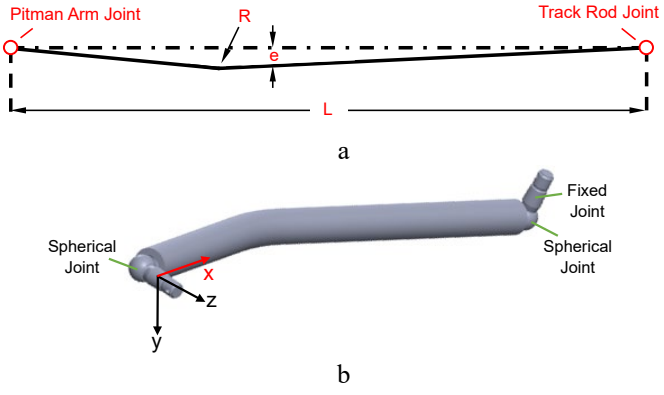


Fig. 11. a. Design of Experiments (DoE) model and Input Parameters: radius (R), eccentricity (e), and rod wall thickness (t), b. The model for the DoE study

In the initial stage, FEA was applied to the primary model, as shown in Figure 10, considering the specified boundary conditions and loading conditions. The load condition used for the analysis is the total moment that the pitman arm must overcome, calculated with the help of Figure 2. The boundary conditions of the parameters were determined according to the working envelope of the wheel and buckling safe design criteria. Here, the drag link is subjected to compressive stress as expected. From the analysis results, equivalent stress and total deformation were selected as the output parameters. The flowchart of the DoE process applied to the component was shown in Figure 12 [23]. Subsequently, a table containing design samples generated by the system using the DoE method for the allowed value range of introduced input parameters was created. The optimisation was performed using ANSYS Workbench® software. Central Composite Design (CCD), which is available as an option in the design table definition of DoE module, was applied to determine the appropriate parameter values [24]. A broad theoretical explanation of this procedure can be found in [25] and [26].

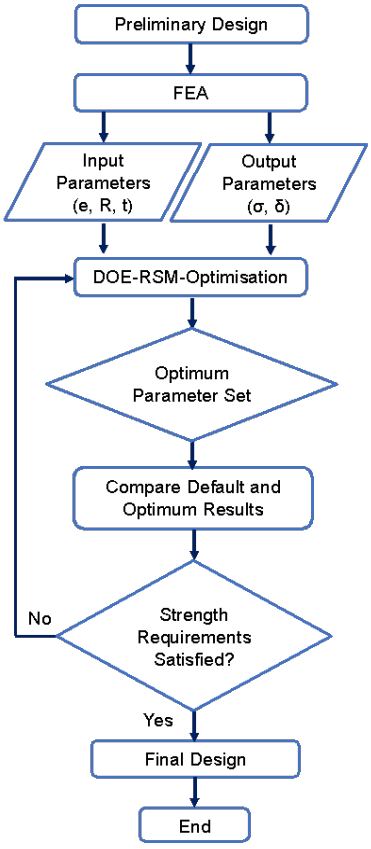


Fig. 12.The flowchart of the DoE [According to [23]]

RS graphs of the output parameters obtained from the system using these input parameters were generated as shown in Figure 13.

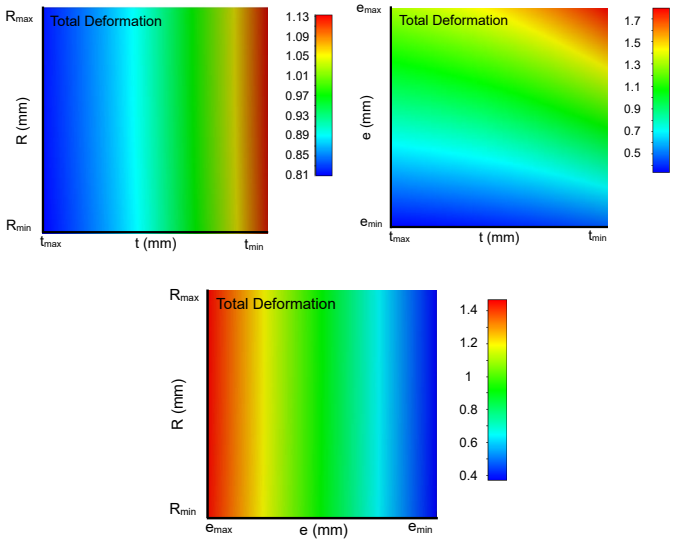


a

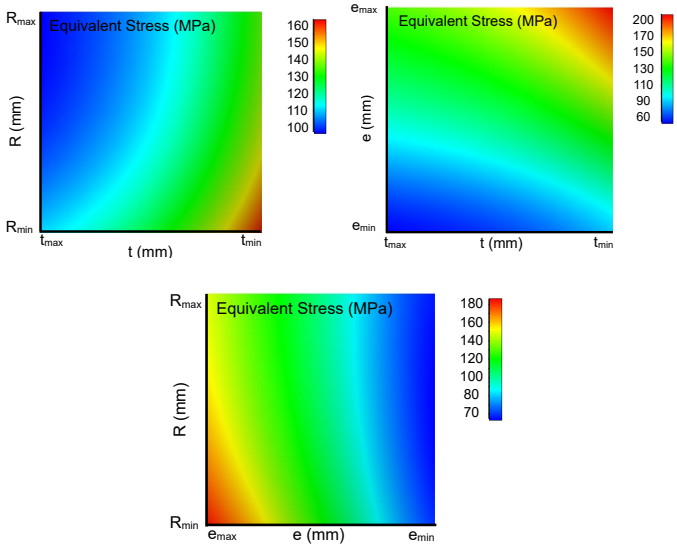


b

Fig. 13. Response surfaces of the parameters, a- concerning Total Deformation, b- concerning Equivalent Stress

In the optimisation module, the constraint that minimises the equivalent stress was determined as the design objective and candidate points were found. These three candidate points generated by the software are given in Figure 14(a). In summary, minimising the stress is an objective function for this parametric study and there are no constraints for this objective function. Because DoE analyses have shown that part designs with different versions of the parameters do not exceed the material yield stress limit, all part designs are in the safe range.

The objective is to find the parameters that give the minimum stress on the part and to find the effect percentages of the design parameters that affect this objective. In order to compare the maximum stress concentration value in the DoE result, FEA analysis was performed on the reconstructed model with optimum parameter values. According to the results shown in Figure 14(b), it is seen that the error rate does not exceed 1%.

| Name | P5 - Equivalent Stress Maximum (MPa) |
|---|---|
| Candidate Point 1 | ★★ 55,775 |
| Candidate Point 2 | ★★ 55,801 |
| Candidate Point 3 | ★★ 55,862 |

a

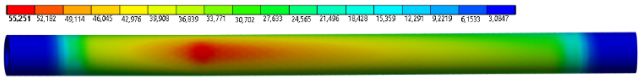

b

Fig. 14. a. Candidate points, b. Validation analysis with the values of these candidate points

Within the scope of the study, the effects of the determined input parameters on the output parameters were also examined. The graph showing the local sensitivity of input parameters for the selected equivalent stress and total deformation output parameters is presented in Figure 15. In terms of component design, the factor that has the highest effect on stress and deformation is eccentricity. This result is in agreement with the literature results for different vehicle components [3]. The safety condition of the new design created with the optimal parameter values were also examined for buckling. It was observed that the component remains in the safe region according to Figure 8.

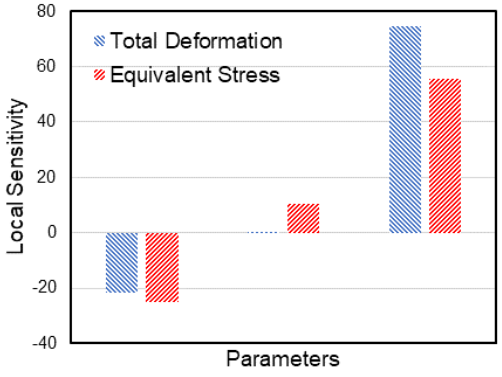


Fig. 15. Local sensitivity (%) of the effect on total deformation and equivalent stress

## 4. Conclusion

This study focuses on examining the effects of various parameters, particularly on the total deformation and stress concentration of a drag link. Finite Element Analysis (FEA) was used to evaluate stress and deformation under loading conditions. For this purpose, a model of the steering linkage was created using the SolidWorks®

commercial software, and the analysis was performed with the ANSYS® Workbench™ 2020 R1 Finite Element software under specified loading conditions. The initial design was made in the form of a hollow rod eccentricity. Result of the analyses showed that, the right turn scenario, which showed the maximum alteration in stress values according to the angular position of the Pitman's arm, was the most critical. Subsequently, a Design of Experiments (DoE) -based optimisation procedure was used to investigate the effects of design parameters such as fillet radius R, eccentricity e, and rod thickness t on the output parameters namely equivalent stress σ and total deformation δ.

The minimum value of eccentricity on the part was determined through the American Institute of Steel Structures criterion (AISC)-based buckling calculations. Response Surface plots were created to determine the relationships between input and output parameters. Subsequently, the obtained parameters were used to re-analyse the DoE results, and it was confirmed that the error was below 1%. Thus, the analysis model's accuracy and reliability in examining the part's behaviour based on the selected parameters were observed. Additionally, it was observed that the parameters obtained from the DoE indicated that the newly designed part is within a safe region against buckling.

When examining the local sensitivity percentages of the parameters on total deformation, it was observed that the eccentricity (e) parameter has the largest effect with an approximate positive rate of 74%. While the fillet radius (R) showed almost negligible influence, the thickness parameter (t) had a negative impact of approximately 20%. The results provide insights into the influence of design parameters on the performance of the part, summarizing the steps for developing an improved part design with structural integrity.

## Acknowledgment

The authors acknowledge to BMC Automotive Industry and Trade Inc. for the technical support they provided. The technical material presented in this study is published with the permission of BMC Automotive Industry and Trade Inc. Some technical details of the system are not given in the study due to the confidentiality policy of BMC Automotive Industry and Trade Inc.

## Conflict of Interest Statement

The authors declare no conflicts of interest.

## CRediT Author Statement

**Kübra Polat**: Methodology, Writing - original draft, Formal analysis
**Mehmet Murat Topaç**: Conceptualization, Methodology, Writing - review & editing, Supervision,
**Ufuk Çoban**: Data curation, Formal analysis

## References

[1] Jazar RN. Vehicle dynamics. Berlin/Heidelberg, Germany: Springer; 2008.

[2] Rill G. Vehicle Dynamics. Lecture notes; 2009.

[3] Topaç MM, Tanrıverdi A, Çolak O, Bilal L, Maviş M. Analysis of The Failure Modes and Design Improvement of an Eccentrically Loaded Connecting Rod for a Double Front Axle Steering Linkage Prototype. Engineering Failure Analysis. 2021; 122: 1052-04. https://doi.org/10.1016/j.engfailanal.2020.105204

[4] Vijaykumar V, Anand P. Design Optimization of Suspension and Steering Systems for Commercial Vehicles. In: Proceedings of ICDMC 2019: Design, Materials, Cryogenics, and Constructions. Springer Singapore. 2020; p. 129-142. https://doi.org/10.1007/978-981-15-3631-1_13

[5] Kılınç I, Toros S. Investigation of The Effect of Bending Process on Fatigue Life and Mechanical Strength of Heavy Commercial Vehicle Drag Links. Eurasian Journal of Science Engineering and Technology. 2022;3.2: 91-102. https://doi.org/10.55696/ejset.1195927

[6] Patil MA, Chavan D, Ghorpade MKUS. FEA of Tie Rod of Steering System of Car. International Journal of Application or Innovation Engineering and Management.2013; 2.5: 222-227.

[7] Okur MZ, Bircan DA. Design and Simulation of A Heavy-Duty Vehicle Steering Component by Analytic and FEA Method. Eurasian Journal of Science Engineering and Technology. 2021; 2.1: 1-9.

[8] Nazaruddin N, Adhitya M, Sumarsono DA, Siregar R, Heryana G, Prasetya S. Static Analysis for the Development of the Steering Mechanism System in the Large Bus as a Preliminary Study for Conversion of Hydraulic Power Steering to Electric Power Steering. In; AIP Conference Proceedings. 2021 September; Vol. 2376, No. 1. https://doi.org/10.1063/5.0064487.

[9] Kurna S, Jain S, Raja P, Vishwakarma L. Truck Steering Component and Linkages Analysis Using Finite Element Method. SAE Technical Paper. 2017; 01-1478. https://doi.org/10.4271/2017-01-1478.

[10] Özmen B, Topaç MM. Effect of Damping Rate on Fatigue Failure Tendency of a Topology-Optimised Swing Arm for a Heavy Commercial Truck Cab Suspension. Engineering Failure Analysis. 2022 ;137: 106276. https://doi.org/10.1016/j.engfailanal.2022.106276

[11] Sharp RS, Granger R. On Car Steering Torques at Parking Speeds. Proceedings of the Institution of Mechanical Engineers, Part D: Journal of Automobile Engineering. 2003; 217.2: 87-96. https://doi.org/10.1177/095440700321700202

[12] Topaç MM, Karaca M, Atak M, Deryal U. Response Surface-Based Design Study of a Relay Lever for a Bus Independent Suspension Steering Mechanism. International Journal of Automotive Engineering and Technologies. 2017:1-10.

[13] Topaç MM, Bahar İ, Kuralay NS. Mass and Stress Optimisation of a Multi-Purpose Vehicle Front Axle Differential Housing for Various Driving Conditions. DÜBİTED. 2016;4(2):501-13. (In Turkish with an abstract in English)

[14] Topaç MM, Duran İ, Kuralay NS. Kinematic Optimisation of the Steering Trapezoid of a 4WD Vehicle by Using Design of Experiments Approach. DUBİTED. 2016;4(2):514-27. (In Turkish with an abstract in English)

[15] Popov EP. Mechanics of Materials.2nd ed. Englewood Cliffs, N.J.: Prentice-Hall, Inc.; 1976.
[16] Shigley JE, Mischke CH. Mechanical Engineering Design. McGraw-Hill; 1989.
[17] Beer F, Johnston EJ, Dewolf J, Mazurek D. Mechanics of Materials. McGraw-Hill ;2012.
[18] Oz Y, Ozan B, Uyanik E. Steering System Optimization of a Ford Heavy-Commercial Vehicle Using Kinematic & Compliance Analysis. SAE Technical Paper, 2012; 2012-01-1937. https://doi.org/10.4271/2012-01-1937.
[19] Doğan O, Kalay O, Kartal E, Karpat F. Optimum Design of Brake Pedal for Trucks Using Structural Optimization and Design of Experiment Techniques. Int J Automot Sci Technol. 2020;4(4):272-80. https://doi.org/10.30939/ijastech..783552.
[20] Güleryüz İC. Lightweight Design of a Torque Plate of Z-Cam Drum Brake for Heavy Duty Vehicles. Int J Automot Sci Technol. 2019;3(2):42-50. https://doi.org/10.30939/ijastech..568059.
[21] Amago, T. Sizing Optimization Using Response Surface Method in FOA. R&D Review of Toyota CRDL.2002; 37.1: 1-7.
[22] Hilgers M, Achenbach W. Chassis and Axles. Berlin: Springer Vieweg ;2021.
[23] Aydın M, Ünlüsoy, YS. Optimization of Suspension Parameters to Improve Impact Harshness of Road Vehicles. The International Journalof Advanced Manufacturing Technology.2012; 60: 743-754. https://doi.org/10.1007/s00170-011-3589-7
[24] Aydın, M., & Ünlüsoy, Y. S. Optimization of Suspension Parameters to Improve Impact Harshness of Road Vehicles. The International Journal of Advanced Manufacturing Technology. 2012,60:743-754. https://doi.org/10.1007/s00170-011-3589-7
[25] D. C. Montgomery, Design and Analysis of Experiments. 5th Ed. Hoboken, New Jersey, John Wiley & Sons, 2000.
[26] R. H. Myers, D. C. Montgomery, C. M. Anderson-Cook, Response Surface Methodology, Process and Product Optimization Using Design of Experiments, 3rd Edition. Hoboken, New Jersey: John Wiley & Sons, 2009